2014 IEEE International Conference on Robotics & Automation (ICRA)
Hong Kong Convention and Exhibition Center
May 31 - June 7, 2014. Hong Kong, China

An Optimized Perching Mechanism for Autonomous Perching with a Quadrotor*

Wanchao Chi, K. H. Low, *Member, IEEE,* K. H. Hoon, and Johnson Tang

***Abstract*— A two-dimensional perching model is proposed first for perching with quadrotors. Then a perching mechanism by means of grasping is designed based on the model. The kinematic specifications of the perching mechanism are optimized to maximize the force transfer ratio so that sufficient grasping force can be generated for reliable perching. A controller of the gripper based on the control strategy from previous development is designed for autonomous perching with a quadrotor. Experiments on the grasping capability and reliability of the mechanism and its effectiveness with the controller for autonomous perching are conducted. Results show that the perching mechanism can generate sufficient grasping force and achieve autonomous perching to a target pole with a quadrotor both effectively and reliably.**

I. Introduction

Research on perching first emerged in the field of ornithology ever since 19th century [1][2][3][4]. With the fast development and vast applications of UAVs in last decade, perching with a UAV has become a booming topic, especially in the field of biomimetics. Nowadays, many disciplines are involved in investigations on perching, including ornithology, biomechanics, aerodynamics, control and mechanical design. Researchers in these fields have obtained fruitful results.

Anatomy structures of birds and their principles have been the main topics in perching-related ornithology research. The concept of automatic perching mechanism (APM), consisting of an automatic digital flexor mechanism (ADFM) and a digital tendon locking mechanism (DTLM), is widely accepted now [5]. The ADFM is activated when birds perch. Their knees and ankles are bent under body weight and the tendon going all along the thigh to the digits is then stretched and the digits will be pulled to grip the perch passively [6]; The DTLM will latch the tendon when gripping is done to secure the grasp without exerting any muscular effort [7][8]. On the other hand, the interactions between birds and environments during perching was left unaddressed until Fisher in 1956 first investigated the interaction dynamics between perching pigeons and the perch by utilizing a mechanical force plate to measure the landing and taking off forces applied by pigeons' legs [9][10]. His research provided a new perspective toward the biomechanics behind birds' perching behaviors, which is rather valuable. Heppner and Anderson further designed a perch integrated with simple force-sensing elements to gauge the taking off thrust exerted by pigeons' legs in [11]. With strain gauges Bonser and Rayner implemented a novel force-transducing perch capable of measuring both magnitude and direction of forces in [12]. The thrusts exerted by legs in time domain was measured and studied, and the force angles were further taken into account. Similar methodology was also adopted by Green and Cheng in [13] where they specifically looked into the factor of kinetic energy of birds during perching. Both kinematic and dynamic variables, such as approaching trajectory, speed and force, were recorded simultaneously for analysis. The authors' perspective from kinetic energy broadens the parameter scope involved in birds' perching, and they also proposed some more parameters for future investigations.

Since it takes a series of aerodynamic maneuvers for birds to perch successfully, the aerodynamic control is a hot spot in the field of perching with UAVs. Wickenheiser and Garcia studied the longitudinal dynamics of a morphing aircraft to achieve the capability of perching in [14]. They further optimized the trajectories for perching in [15]. Main efforts were made on aerodynamic analysis and its control strategy. Cory and Tedrake researched aerodynamic control for maneuvers at high angles-of-attack in [16]. They developed a particular procedure to perch a small fixed-wing glider with an aggressive high angle-of-attack. Roberts *et al*. further studied the controllability of fixed-wing perching with a simplified closed-form model [17]. Their results showed that additional actuations can facilitate perching with less control effort. Mellinger also investigated trajectory generation and control of quadrotors for aggressive maneuvers [18]. Perching is one of the potential maneuvers that they are aiming at, as their studies in [19].

Anderson *et al*. proposed several feasible concepts for perching with UAVs, and mainly studied the use of sticky pads in [20]. Kovac *et al*. designed a practical mechanism for gliders to perch on vertical surfaces using torsion springs and needles in [21]. It worked rather well even with concrete walls. Desbiens *et al*. also developed a perching mechanism that is able to perch a fixed-wing UAV to a vertical wall using micro-spines [22][23]. Their design is innovative, but it requires aggressive maneuvers of the UAV. Doyle *et al*., for the first time, applied bio-inspired compliant gripping and passive perching to a quad-rotor [24][25]. This concept is closer to birds' perching in terms of biomimetics, but integrated perching experiments with quadrotors were not sufficiently addressed. Nagendran *et al*. proposed a leg concept and corresponding control strategies for UAV perching [26]. The leg mechanism is inspired directly from the typical anatomy of a bird's leg. However, no prototype had been developed and evaluated. Recent work by Pu Xie *et al*.

*Resrach collaborated with DSO, Singapore.

Wanchao Chi, K. H. Low and K. H. Hoon are with School of Mechanical and Aerospace Engineering, Nanyang Technological University, 639798 Singapore (e-mail: wchi1@e.ntu.edu.sg; mkhlow@ntu.edu.sg; mkhhoon@ntu.edu.sg).

Johnson Tang is with the Defence Science Organization, Singapore (e-mail: tjohnson@dso.org.sg).

addressed the bio-inspired control strategy of perching with a quadrotor based on the *Tau theory* [27]. Dynamics and control of the quadrotor were taken into account and promising simulation results were obtained. It's a big step toward a bio-inspired perching methodology for UAVs, although validation with a hardware prototype is still underway.

It can be seen that no comprehensive biomechanics model of birds' perching has been established yet, though research on perching in ornithology have already addressed general fundamentals. Also, to our best knowledge, an interaction model of the perching system with a gripping end effector hasn't been proposed in existing perching mechanism development, although grasping in industrial robots has been well studied [28][29][30][31]. In light of this, the authors, in the previous paper [32], summarized the research on anatomy structures of birds involved in perching systematically and further generalized the perching procedure of birds into three stages, providing fundamental guidelines for perching mechanism development and control strategy design. Recently we further presented a control strategy based on the generalized perching procedure for autonomous perching with a quadrotor in [33]. As parallel investigations, in this paper the interaction model of perching UAVs is addressed in Section II, then design and optimization of the grasping-based perching mechanism are presented in Section III, and a new controller of the gripper for autonomous perching with a quadrotor is designed in Section IV. In Section V experiments on both static and dynamic grasping of the perching mechanism and on autonomous perching of the whole system with a quadrotor are conducted and results are analyzed. Finally, conclusions are drawn in Section VI.

II. TWO-DIMENSIONAL PERCHING MODEL

A perching model for force analysis covering the target, the perching mechanism and the UAV platform is definitely necessary for perching mechanism development. We therefore start with modeling of such interactions.

Several conditions are prescribed as follows. Firstly, quadrotors are taken as the UAV platform since they not only are more agile in terms of aerial manipulation but also can carry larger payloads compared to fixed-wing UAVs and ornithopters of similar size. Secondly, the configuration of the perching mechanism is supposed to be symmetric about longitudinal and lateral planes as a quadrotor is. Thirdly, a gripping mechanism mimicking birds' foot is chosen as the end effector for perching. Certainly a gripper cannot suit all potential perching circumstances, for instance, vertical surfaces, but it works with most common perch in nature such as tree branches, roofs and ground. This is also why a cylindrical pole fixed to ground reference frame, approximating tree branches, is adopted as the target perch in the investigations. Moreover, envelop grasping with form closure and frictional point contacts from grasping of industrial robots [28] are also assumed. Consequently, the conditions above lead to a simplified two-dimensional perching model in the longitudinal plane, as shown in Figure 1.

The mass of the quadrotor is represented by M. The perching mechanism consists of a gripper, which outputs grasping forces F_g to the target (F_g' in Figure 1 denotes reaction forces of F_g) via a pair of digits, and the frame structure, which keeps the center of gravity of the quadrotor a distance of H from the grasping center. To derive form-closure grasp, the digit is assumed to have a curvature with a certain angle φ. Two contact points exist between each digit and the target of diameter d, and F_g is in the direction of the bisector of φ as the resultant force. Friction forces applied to the perching mechanism at contact points are represented by f_i, i=1,2,3,4. In the 2D model only a pair of digit is considered for simplification, although two pairs are needed in reality to gain lateral balance of the quadrotor. Furthermore, a horizontal disturbance force F_d simulating wind disturbance is imposed to the quadrotor to generalize the model. At the same time a misalignment angle θ exists between the orientation axis of the perching mechanism and the vertical axis of ground reference frame. F_{gf} denotes the reaction force of G and F_d.

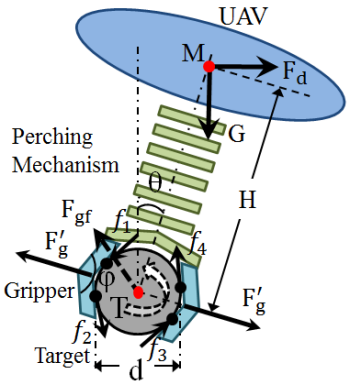

Figure 1. Two-dimensional Perching Model of a UAV system

It is obvious from the model that the balance of the whole system is maintained by the torque T derived from the friction forces f_i. As the quadrotor is able to hover as a helicopter, a less aggressive perching trajectory, following which the quadrotor flies horizontally to the above of the target and descends gradually to the target, is adopted. Consequently only static friction case is considered, and all friction forces f_i are assumed to be equal. Note that such a 2D model is still applicable to dynamic analysis of perching as long as dynamic properties are associated to every single degree of freedom respectively.

Based on the assumptions above, the static moment equilibrium equation and the relation between f_i and F_g can then be written as

$$MgH\ sin\theta + F_d H cos\theta = T = \frac{d}{2}\sum_{i=1}^{4} f_i, \quad (1)$$

$$f_i \le \mu F_g / (2sin\tfrac{\varphi}{2}), \mathrm{i} = 1,2,3,4, \quad (2)$$

where μ is the static friction coefficient between the digits and the target. Therefore, in the critical case where f_i reaches the maximum, it can be obtained that

$$F_g = \frac{Hsin\frac{\varphi}{2}}{\mu d}(Mgsin\theta + F_d cos\theta). \quad (3)$$

The quadrotor utilized weighs around 1.3kg, including the battery. Taking the possible extra weight of the perching mechanism into account, it is reasonable to prescribe the mass of the UAV, M, to be 1.8kg. With the geometry of the quadrotor known, the disturbance force F_d due to sideway wind is estimated to be 1N, the distance H is assumed to be

0.15m and the diameter d of the target is set as 0.1m. The maximum misalignment angle θ_{max} is prescribed to be 30° for the safety of the UAV, and the digit curvature angle φ is assumed to be 140° to achieve envelop grasp. The coefficients of static friction between wood and some common materials range from 0.2 to 0.8, while those between rubber and common materials are mostly larger than 0.4 [34]. As rubber is supposedly to be applied to the digits, a conservative value of 0.4 is estimated for the coefficient of static friction μ. Consequently parameters assumed are listed in TABLE I.

TABLE I. ASSUMED VALUE OF MODEL PARAMETERS

M (kg)	F_d (N)	θ_{max} (degree)	H (m)	φ (degree)	d (m)	μ
1.8	1	30	0.15	140	0.1	0.4

Submitting the values above into (3) derives that the required grasping force F_{gr} is 34.1N. Assuming the actuation force results from the output torque T_o of a servo with a common horn length (L_h) of 2 to 4 cm, the following requirement of the servo can be further obtained.

$$T_o \geq T_{max} = 2F_{gr} \cdot \max\{L_h\} \approx 27.3 \text{ kgf} \bullet \text{cm} \quad (4)$$

Therefore a Futaba servo of max output torque T_{omax} of 37 kgf•cm is employed. To establish a design reference, the force transfer ratio of the perching mechanism is defined as follows based on the 2D perching model.

$$\lambda = \frac{2F_g}{F_a}, \quad (5)$$

where F_a is the actuation force from the actuator. Therefore the estimated force transfer ratio λ_e of the perching mechanism can be derived as

$$\lambda_e \geq \frac{2F_{gr}}{F_a} = \frac{T_{max}}{T_{omax}} \approx 0.74. \quad (6)$$

III. PERCHING MECHANISM DESIGN

A. Force Amplification

Force amplification can be defined as a process with force transfer ratio larger than one. For a perching mechanism using gripping method, the larger the grasping forces it can generate, the larger the friction forces there could be to secure the perching status. Force amplification can thus benefit the performance of the perching mechanism significantly by increasing its force transfer ratio. A force amplifying concept in Figure 2 is applied.

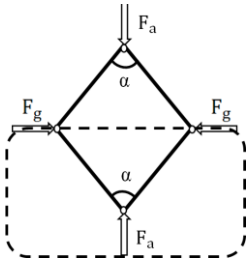

Figure 2. The Force Amplifying Concept

If two pairs of force are applied to the four joints of a rhombic four-bar linkage symmetrically as depicted in Figure 2, the transfer ratio from F_a to F_g can be expressed as

$$\lambda_0 = \frac{2F_g}{2F_a} = tan\frac{\alpha}{2}. \quad (7)$$

It's obvious that $\lambda_0 > 1$ when 90°<α≤180°. Moreover, as α increases to 180°, λ_0 tends to become infinite. This characteristic of force amplification is therefore used for the perching mechanism. To simplify the mechanism, only half of the rhombic linkage (the part enclosed by dashed lines in Figure 2) is utilized in our design. Note that such a simplification has no effect on λ_0 and F_a can be balanced by vertical reaction forces at the joints where F_g is outputted.

B. Kinematic Optimization of the Gripping Mechanism

Taking into account the design reference λ and making use of the force amplifying concept, a gripping mechanism is designed as in Figure 3. The actuation force generated by the servo is transmitted to the gripping digits via the shaft constrained to vertical linear motion and the transmission arms which in pairs form a force amplifier of half rhombic configuration. The force transfer ratio of the mechanism should be maximized via kinematic optimization.

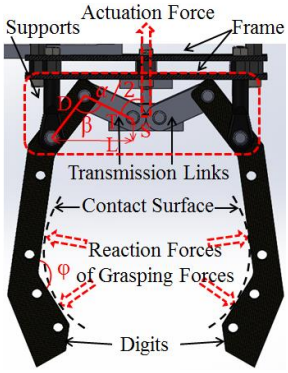

Figure 3. The gripping mechanism for perching (adopted from [33])

The gripping mechanism is based on four-bar linkages which consist of actuation shaft, transmission arm, digit and the frame. Therefore a kinematic diagram is drawn in Figure 4 for analysis. The origin of the reference frame is set to the fixed joint. The slider is constrained to vertical linear motion, serving as the input link, and its coordinate is (L, S) where L is constant and S is variable. The lengths of the output link, i.e., the digit, and the coupler link, i.e., the transmission arm, are represented with D and T respectively. The angle α/2 between the transmission arm and vertical axis is defined as the input angle, the angle β between the digit and the transmission arm denotes the coupling angle, and the angle γ between the digit and x axis is defined as the output angle.

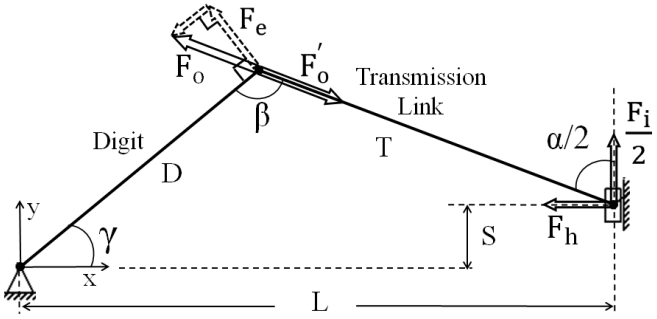

Figure 4. Kinematic diagram of the gripping mechanism

In Figure 4, the input actuation force is denoted by $F_i/2$, while the output force transmitted to the digit is represented by F_o. F_o' is the reaction force of F_o applied to the transmission link, and F_h is the horizontal squeezing force. As the digit can only rotate, the effective output force, F_e, can be expressed as

$$F_e = F_o \sin(\pi - \beta) = F_o \sin\beta = \frac{F_i \sin\beta}{2\cos\frac{\alpha}{2}}. \quad (8)$$

Therefore the force transfer ratio is

$$\lambda = \frac{F_e}{F_i/_2} = \frac{\sin\beta}{\cos\frac{\alpha}{2}}. \quad (9)$$

To maximize λ, β should be maintained in the neighborhood of 90^o and α should be as close to 180^o as possible. As both β and α vary with respect to the position input S, their relations with S are first derived.

Based on the geometry of the mechanism in x and y directions, the equations below can be obtained.

$$\begin{cases} D\sin\left(\beta - \frac{\alpha}{2}\right) + T\sin\frac{\alpha}{2} = L \\ D\cos\left(\beta - \frac{\alpha}{2}\right) - T\cos\frac{\alpha}{2} = S \end{cases}. \quad (10)$$

Eliminating α and β separately yields the equations below.

$$\cos\beta = \frac{D^2+T^2-S^2-L^2}{2DT}, \quad (11)$$

$$\cos\left(\frac{\alpha}{2} - \phi\right) = \frac{D^2-T^2-S^2-L^2}{2T\sqrt{S^2+L^2}}, \quad (12)$$

where ϕ satisfies $\tan\phi = \frac{L}{S}$. These relationships can also be derived from the triangle, consisting of D, T and the side from the origin to the slider, by using the law of cosines.

Taking the dimensions of the quadrotor utilized into account, L is prescribed to be 35mm. Due to the limit of the mechanism height H, D is set to be 20mm. Moreover, the range of input S is limited to [-7, 12] mm which is the applicable workspace for the actuation shaft. Hence, λ is reduced to be a function of S and T, and only T needs to be determined. An accumulated force transfer ratio λ_a is further defined as

$$\lambda_a(T) = \int_{S_{min}}^{S_{max}} \lambda(S,T)\, dS. \quad (13)$$

Given a constant actuation force F_a, λ_a reflects the overall effectiveness of force amplification over the workspace of S with different T. Also, it covers the influence of different target diameter d, as individual S corresponds to individual d. To identify the constraints imposed on T, the range of cosβ is considered. Obviously, $-1 < \cos\beta < 1$. It can thus be obtained from Eqn. (11) that

$$\sqrt{|S|_{max}^2 + L^2} - D < T < \sqrt{|S|_{min}^2 + L^2} + D. \quad (14)$$

Furthermore, two cases of singularity, in which α reaches 180^0 before S reaches the maximum position or β reaches 180^0 when S is maximum, and one extreme case, in which γ reaches 90^0 when S is maximum, are considered. See Figure 5.

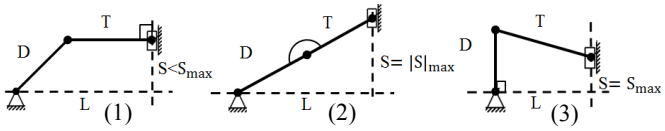

Figure 5. Three extreme cases for constraints of T. (1): singularity of α; (2): singularity of β; (3): maximum γ.

The corresponding constraints on T can therefore be derived as below.

For α:

$$L - \sqrt{D^2 - S_{max}^2} < T < L + \sqrt{D^2 - S_{max}^2}, \quad (15)$$

For β and γ:

$$\sqrt{L^2 + S_{max}^2} - D < T < \sqrt{(D - S_{max})^2 + L^2}, \quad (16)$$

Consequently, the optimization problem can be expressed as

Objective: Maximize $\lambda_a(T)$,

Subject to: $S \in [S_{min}, S_{max}]$, Inequalities (14), (15) and (16).

The optimization problem defined above is investigated numerically using Matlab. S and T are discretized first within their constraint ranges, and values of λ_a with different values of T_i are then calculated and illustrated in Figure 6. It's obvious that the maximum of λ_a corresponds to $T_1 = 0.02$m. The force transfer ratio λ in this case with respect to S is further calculated and shown in Figure 7. It shows that the force transfer ratio is already larger than 1 at the initial position and it increases gradually to almost 12 at the maximum input position. Such a characteristic is consistent with the fact that the smaller the diameter of the target is, the larger the grasping force is needed to generate the balancing moment for the quadrotor, and will therefore greatly benefit the grasping performance of the perching mechanism. The initial force transfer ratio of 1.3 is still acceptable since the impact at the beginning of perching will facilitate the grasping, resulting in less actuation force required from the motor. The maximum force transfer ratio of 12 is rather promising, with combination of a powerful motor.

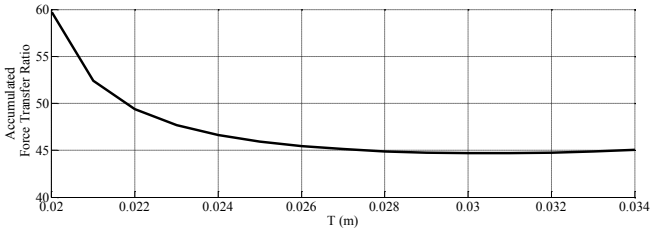

Figure 6. Accumulated force transfer ratio λ_a under different lengths of T

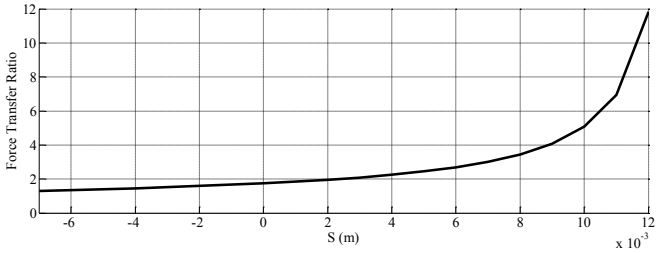

Figure 7. Force transfer ratio λ under the optimal $T_i = 0.020$m

As the digit is a solid link that works as a lever about its pivot joint, it introduces a constant force transfer ratio K into the force transmission loop. K can be determined according to the workspace required for various applications. The overall force transfer ratio λ_{tot} for the perching mechanism can further be written as

$$\lambda_{tot} = K\lambda = K\sin\beta/\cos\frac{\alpha}{2} \quad (17)$$

As impact happens during perching, the perching mechanism is supposed to be strong enough to withstand it. Another critical issue of perching with UAVs is the weight of the mechanism, or payload capacity of the UAVs. In the case of perching, the less the perching mechanism weighs, the more agility in manipulation it will give the UAV, which will significantly benefit the whole perching system. Therefore, carbon fiber sheets are utilized for the mechanism frame and the digits to increase the strength of the whole structure and also reduce its weight. Nylon spacers are employed to support the frames, and Delrin shafts are designed for all the revolute joints. As a result, the mechanism, including the servo, weighs only about 350g which is far within the payload capacity of the quadrotor used. See Figure 8 for the final perching mechanism that is designed and fabricated. Two pairs of the gripping mechanism are employed such that effective grasp is guaranteed and lateral stability of the quadrotor is secured.

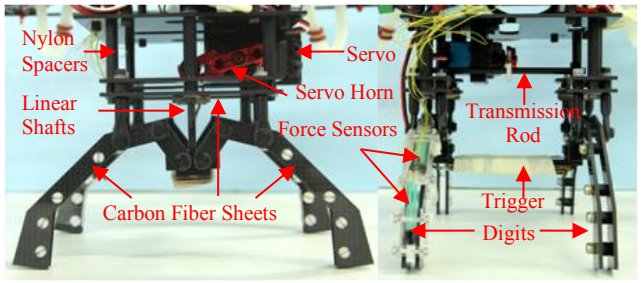

Figure 8. Final version of the perching mechanism (left: lateral view; right: front view.)

IV. Controller Design for Autonomous Perching

Some drawbacks of the previous controller [33] were found during perching experiments. For instance, duty cycle is tuned instantly to the target position with respect to the force error. This leads to significant current sinking when force sensor readings are not accurate enough and over-grasping happens. It puts the servo at risk of damage and also decreases the energy efficiency. The controller is redesigned to improve its performance in duty cycle tuning here.

The controller is refined based on the characteristics of the servo. The only parameter of the servo that can be directly controlled is the angular position of its shaft, while the output torque is internally controlled by its own onboard controller. As long as position error exists and the required output torque is within its capability, the actual output torque will be increased automatically. Therefore a threshold F_t of the force feedback from the force sensors can be set as a Boolean indicator of the gripper status. It means the gripper contacts the target and starts grasping it when force feedback exceeds the threshold F_t. The duty cycle D_c should be tuned at the optimal step which makes the servo actuate at the fastest speed when no contact happens; otherwise the step itself should be varied accordingly to the actual grasping force such that grasping under loading can be finished as quickly as possible while avoiding damaging the servo. Consequently, the controller can be expressed as

$$D_c(k) = D_c(k-1) + D_{step}, \tag{18}$$

$$D_{step} = \begin{cases} D_{opt}, & F_g < F_t \\ c_1 \cdot D_{opt} - c_2 \cdot n \cdot \Delta D, & F_t \le F_g \le F_o, \\ 0, & F_g > F_o \end{cases} \tag{19}$$

where $D_c(k)$ is discrete duty cycle value, D_{step} is the step value for tuning the duty cycle, D_{opt} is the optimal step value that leads to the fastest rotation of the servo, ΔD is the resolution of duty cycle for the specific servo, c_1 and c_2 are coefficients that adjust the step value during grasping, $n = 0, 1, 2, \cdots$ and it increases with k. Note that in our case D_{opt} and ΔD are estimated to be 120ms and 10ms according to the datasheet of the servo, and c_1 and c_2 are experimentally determined to be 0.5 and 1.

V. Experiments and Results

With different versions of the perching mechanism during the process of finalization, we perform a series of experiments to assess its grasping ability and reliability of autonomous perching in various scenarios. As mentioned, a tube of diameter 10cm attached to an aluminum frame is utilized as the target pole, and a piece of foam and rubber is coiled around the tube respectively in different experiments to increase the friction coefficient to the estimated value in the model.

A. Static Grasping with the Perching Mechanism Alone

In the experiments of static grasping, a payload is first attached to the gripper, simulating the weight of the quadrotor. Then the gripper is aligned directly over the pole and actuated to grasp the pole completely. While the gripper is maintaining the grasp, we tilt the pole gradually until the gripper slips off. Weights of 1kg and 2kg are utilized in the experiments respectively. Figure 9 depicts the max misalignment angles that the gripper can hold to in the experiments.

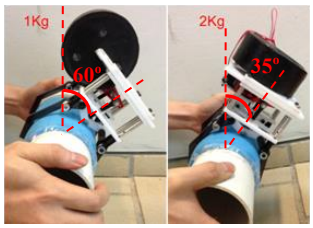

Figure 9. Static grasp under misalignment and payload with the first version prototype (Left: 1kg; Right: 2kg)

It can be seen that with 1kg payload, the gripper can hold up to 60° of misalignment angle, while up to 35° with 2kg payload. The experiment results are generally consistent with the model assumptions. Since a quadrotor which can hover and then descend for perching is utilized as the UAV platform, the misalignment angle is generally supposed to be close to 0°. Therefore, the results reveal that the grasping force generated by the gripper is large enough to secure the quadrotor in general perching circumstances.

B. Dynamic Perching with the Perching Mechanism Mounted to the Quadrotor

Three experiments of dynamic perching with the second version of the gripping mechanism are conducted in our lab, the first being taking off from ground and perching to a target pole, the second being re-launching from the pole and perching again, and the third being re-launching from the pole and perching with a misalignment angle. One more experiment of dynamic perching to a tree is performed in nature. The experiment protocols are illustrated in Figure 10 and Figure 11, respectively. The quadrotor and the perching mechanism are remotely controlled during these experiments.

In experiment 1, the UAV system successfully perches to the pole with the first trial, although only digit tips contacts the pole. It shows that even an incomplete grasp can secure the perching. In experiment 2, the quadrotor stumbles a bit when re-launching, but it manages to release from the pole and take off. Moreover, the perching later is properly performed in terms of alignment with the pole, and a complete grasp is achieved. In experiment 3, the quadrotor succeeds in launching again and it happens to misalign with the pole during perching, leading to a misaligned but complete grasp. The misalignment angle is within the range that the gripper can withstand, so the perching is still reliable.

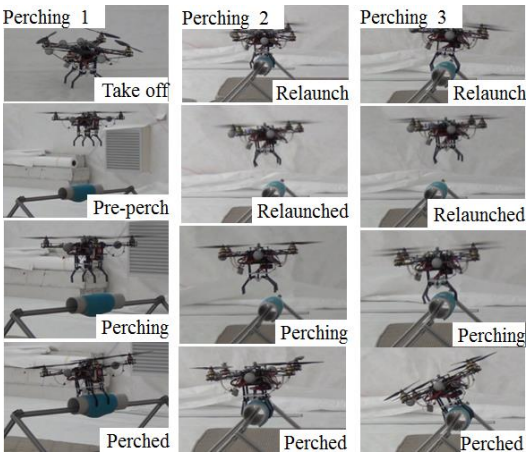

Figure 10. Perching experiments with the quadrotor (left to right: three experiments; top to bottom: procedures of each perching)

In experiment 4, the quadrotor takes off from ground and perches to a tree branch with sufficient clearance to approach and with moderate diameter to grasp. It can be seen that misalignment between the gripper and the tree branch exists and the final perching state is a little off balance in lateral direction. This is because of the error in remote control of the quadrotor and the breeze blowing during the experiment. However, the whole perching procedure is still very smooth and the perching is deemed as reliable since no oscillation of the quadrotor is observed after perched.

Figure 11. Perching to a tree branch (1: Pre-perch; 2: Perching; 3: Perched)

Based on the results we can conclude that the grasping ability and reliability of the perching mechanism during dynamic perching are validated for both lab and nature environments. The perching mechanism designed is effective for remotely-controlled perching with a quadrotor.

C. Autonomous Grasping with the Controller

As the perching mechanism has already been validated to be effective for perching under remote control, we further implement the controller and test its reliability of autonomous grasping. In this experiment the perching mechanism is assembled to a quadrotor and dropped from above the pole. Once triggered, it will grasp the pole autonomously. See Figure 12.

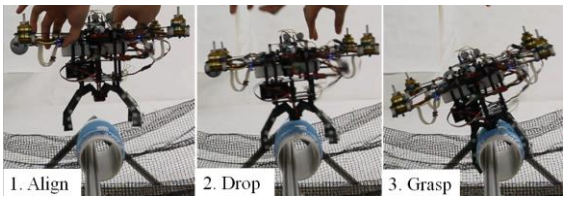

Figure 12. Drop-and-Grasp (1: Align the quadrotor with the pole; 2: Drop the quadrotor; 3: The perching mechanism gets triggered upon impact and grasps autonomously)

The drop-and-grasp test was conducted dozens of times, and the perching mechanism succeeded in grasping the target firmly in most of them. Figure 12 shows a successful grasp even with a certain misalignment angle which is caused by the impact and rebound during engagement with the target. In summary, the performance of the perching mechanism is rather consistent with those in previous manual testing, and the controller is therefore reliable enough for autonomous perching with a quadrotor.

D. Autonomous Perching with a Quadrotor

Experiments on autonomous perching with a quadrotor are conducted after the perching mechanism and the controller are verified. The experimental setup is shown in Figure 13, and is basically the same as that demonstrated in [33]. Note that autonomous control of the quadrotor via VICON motion capture system is implemented by the authors' colleagues, and it is therefore not covered in this paper.

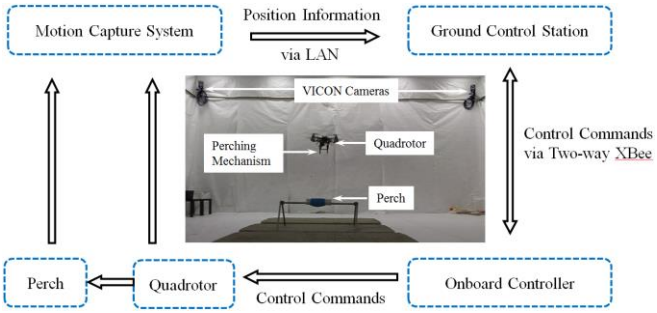

Figure 13. Experimental Setup for Autonomous Perching with a Quadrotor

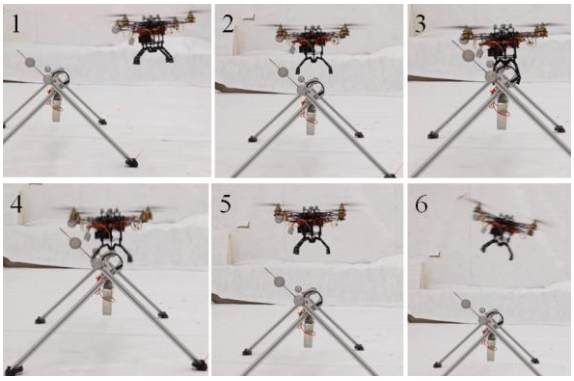

Figure 14. Autonomous perching (1: approaching, 2: aligning and declining, and 3: grasping and perched) and de-perching (4: releasing, 5: rebuilding flight, and 6: fly away)

As shown in Figure 14, the quadrotor autonomously flies to the above of the target and hovers to align. After aligned it descends vertically to perch to the target. The perching mechanism will be automatically actuated to grasp once it's triggered by the target. When reliable perching is achieved the

quadrotor will then shut down. To re-launch the quadrotor, the perching mechanism will release from the target when the lifting force is large enough to rebuild the flight. The autonomous perching is successfully repeated for several times, and failure rarely occurs after initial adjustment of testing setup, which reveals the effectiveness and reliability of the perching mechanism and the controller designed for autonomous perching with the quadrotor.

VI. CONCLUSIONS

In this paper the authors develop an autonomous perching mechanism based on grasping for applications with quadrotors. The 2D perching model is simple, but it provides sufficient support for perching mechanism design. The force transfer ratio of the perching mechanism is maximized by kinematic optimization. A controller for fine tuning the duty cycle of the servo is also designed. Experiments show that the perching mechanism is capable of both perching a quadrotor to and re-launching it from the target pole autonomously, and the perching reliability is guaranteed even under misalignment.

ACKNOWLEDGMENT

The authors would like to thank the Defence Science Organization (DSO), Singapore for its sponsorship to this work. We would also express our gratitude to Zhao Weihua and Chiew Soon Hooi for the reliable quadrotor platform that they provide. Besides, Tan Wee Kiat, Quek Jian Xing and Liang Hongde's contributions are sincerely appreciated too.

REFERENCES

[1] R. Owen, *On the anatomy of vertebrates. II. Birds and mammals*, London: Longman Green, 1866.

[2] M. Watson, "On the mechanisms of perching in birds," *Journal of Anatomy*. Vol. 3, pp. 379-384, 1869.

[3] J. L. Renaut, "Recherches sur las transformation vesiculeuse des elements cellulaires des tendons (Cellules tubulaires de Ranvier)," *Archs Physiol Norm Path*, Vol. 4, pp. 271-191, 1872.

[4] I. Ranvier, "Sur les tendons des doigts chez les oiseaux. J Micrographie. Histologie humaine et comparee. Anatomie vegetale. Botanique. Zoologie. Bacteriologie," *Applications diverses du Microscope*, Vol. 13, pp. 167-171, 1889.

[5] P. Galton, and J. Shepherd, "Experimental analysis of perching in the European starling (Sturnus vulgaris: Passeriformes; passeres), and the automatic perching mechanism of birds," *Journal of Experimental Zoology*, vol. 317, pp. 205-215, 2012.

[6] B. Wilson, *Birds: Readings From "Scientific American"*. San Francisco: W. H. Freeman, 1980.

[7] T. H. Quinn, and J. J. Baumel, "The digital tendon locking mechanism of the avian foot (Aves)," *Zoomorphology*, Vol. 109, pp. 281-293, 1990.

[8] T. H. Quinn, and J. J. Baumel, "Chiropteran Tendon Locking Mechanism," *Journal of Morphology*, Vol. 216, pp. 197-208, 1993.

[9] H. Fisher, "The landing forces of domestic pigeons," *The Auk*, Vol. 73, No. 1, pp. 85-105, 1956.

[10] H. Fisher, "Apparatus to measure forces involved in the landing and taking off of birds," *The American Midland Naturalist*, Vol. 55, pp. 334-342, 1956.

[11] F. Heppner, and J. Anderson, "Leg thrust important in flight take-off in the pigeon," *Journal of Experimental Biology*, Vol. 114, pp. 285-288, 1985.

[12] R. Bonser, and J. Rayner, "Measuring leg thrust forces in the common starling," *The Journal of Experimental Biology*, Vol. 199, pp. 435-439, 1996.

[13] P. Green, and P. Cheng, "Variation in kinematics and dynamics of the landing flight of pigeons on a novel perch," *The Journal of Experimental Biology*, Vol. 201, pp. 3309-3316, 1998.

[14] A. Wickenheiser, and E. Garcia, "Longitudinal Dynamics of a Perching Aircraft," *Journal of Aircraft*, vol. 43, no. 5, pp.1386-1392, 2006.

[15] A. Wickenheiser, and E. Garcia, "Optimization of Perching maneuvers Through Vehicle Morphing," *Journal of Guidance, Control, and Dynamics*, vol. 31, no. 4, pp.815-823, 2008.

[16] R. Cory, and R. Tedrake, "Experiments in Fixed-Wing UAV Perching," *AIAA Guidance, Navigation and Control Conference and Exhibit*, August 2008, Honolulu, USA.

[17] J. Roberts, R. Cory, and R. Tedrake, "On the Controllability of Fixed-Wing Perching," *2009 American Control Conference*, June 2009, Hyatt Regency Riverfront, USA.

[18] D. Mellinger, N. Michael, and V. Kumar, "Trajectory generation and control for precise aggressive maneuvers with quadrotors," *The International Journal of Robotics Research*, vol. 31, no. 5, pp.664-674, 2012.

[19] D. Mellinger, M. Shomin, and V. Kumar, "Control of Quadrotors for Robust Perching and Landing," *International Powered Lift Conference*, October 2010, Philadelphia, USA.

[20] M. Anderson, C. Perry, B. Hua, D. Olsen, J. Parcus, K. Pederson, and D. Jensen, "The Sticky-Pad Plane and other Innovative Concepts for Perching UAVs," *47th AIAA Aerospace Sciences Meeting Including The New Horizons Forum and Aerospace Exposition*, January 2009, Orlando, USA.

[21] M. Kovač, J. Germann, C. Hüurzeler, R. Siegwart, and D. Floreano, "A Perching Mechanism for Micro Aerial Vehicles," *Journal of Micro-Nano Mechatronics*, vol. 5, no. 3, pp. 77, 2010.

[22] A. Desbiens, and M. Cutkosky, "Landing and Perching on Vertical Surfaces with Microspines for Small Unmanned Air Vehicles," *Journal of Intelligent Robot System*, vol. 57, pp. 313-327, 2010.

[23] A. Desbiens, A. Asbeck, S. Dastoor, and M. Cutkosky, "Hybrid Aerial and Scansorial Robotics," *2010 IEEE International Conference on Robotics and Automation*, pp. 1114-1115, 2010.

[24] C. Doyle, J. Bird, T. Isom, J. Johnson, J. Kallman, J. Simpson, R. King, J. Abbott, and M. Minor, "Avian-Inspired Passive Perching Mechanism for Robotic Rotorcraft," *2011 IEEE/RSJ International Conference on Intelligent Robots and Systems*, September 2011, San Francisco, USA.

[25] C. Doyle, J. Bird, T. Isom, J. Kallman, D. Bareiss, D. Dunlop, R. King, J. Abbott, and M. Minor, "An Avian-Inspired Passive Mechanism for Quadrotor Perching," *IEEE/ASME Transaction on Mechatronics*, vol. 18, no. 2, pp. 506-517, Apr. 2013.

[26] A. Nagendran, W. Crowther, and R. Richardson, "Biologically Inspired Legs for UAV Perched Landing," *IEEE A&E Systems Magazine*, vol. 27, issue 2, pp. 4-13, 2012.

[27] P. Xie, O. Ma, and Z. Zhang, "A Bio-inspired Approach for UAV Landing and Perching," *AIAA Guidance, Navigation, and Control (GNC) Conference*, August 2013, Boston, USA.

[28] A. Bicchi, "On the closure properties of robotic grasping," *The International Journal of Robotics Research*, Vol. 14, No. 4, pp. 319-334, 1995.

[29] K. B. Shimoga, "Robot Grasp Synthesis Algorithms: A Survey," *The International Journal of Robotics Research*, Vol. 15, No. 3, pp. 230-266, 1996.

[30] K. B. Shimoga, and A. A. Goldenberg, "Soft Robotic Fingertips Part II: Modeling and Impedance Regulation," *The International Journal of Robotics Research*, Vol. 15, No. 4, pp. 335-350, 1996.

[31] C. Lanni, and M. Ceccarelli, "An Optimization Problem Algorithm for Kinematic Design of Mechanisms for Two-Finger Grippers," *The Open Mechanical Engineering Journal*, Vol. 3, pp. 49-62, 2009.

[32] W. Chi, K. H. Low, K. H. Hoon, J. Tang, and T. H. Go, "A Bio-inspired Adaptive Perching Mechanism for Unmanned Aerial Vehicles," *Journal of Robotics and Mechatronics*, vol. 24, no. 4, pp. 642-648, 2012.

[33] W. Chi, K. H. Low, K. H. Hoon, and J. Tang, "Design of Control Strategy for Autonomous Perching with a Quadrotor," *The 4th International Conference of Bionic Engineering*, August 2013, Nanjing, China.

[34] Engineer's Handbook (2013), Reference Tables [Online]. Available: http://www.engineershandbook.com/Tables/frictioncoefficients.htm